Catalysis Today 142 (2009) 196–201

Contents lists available at ScienceDirect

Catalysis Today

journal homepage: www.elsevier.com/locate/cattod

A novel multi-channel reactor system combined with operando UV/vis diffuse reflectance spectroscopy: Proof of principle

M.J.G. Fait *, R. Abdallah [1], D. Linke, E.V. Kondratenko, U. Rodemerck

Leibniz Institute for Catalysis at Rostock University, Branch Berlin, Richard-Willstätter-Str. 12, D-12489 Berlin, Germany

ARTICLE INFO

Article history:
Available online 5 December 2008

Keywords:
High-throughput experimentation
Oxidative dehydrogenation
Propene
Propane
UV/vis diffuse reflectance spectroscopy
Operando methodology

ABSTRACT

A 36 channel reactor system combining high-throughput experimentation (HTE) with operando UV/vis diffuse reflectance (UV/vis-DR) spectroscopy is introduced and applied for the oxidative dehydrogenation of propane (ODP) to propene at 500 °C over polycrystalline V_2O_3, VO_2, and V_2O_5. This set-up enabled to monitor reaction-induced reduction of V_2O_5 to V_2O_3, and VO_2 during the ODP reaction. The operando UV/vis-DR spectroscopic analysis along the catalyst bed demonstrated that the vanadium oxidation state at the reactor inlet is higher than at the reactor outlet. This is due to the depletion of oxygen and the enrichment of propene down stream along the catalyst bed.

1. Introduction

High-throughput experimentation (HTE) for the development and optimisation of heterogeneous catalysts was introduced in the middle of the 1990s by Symyx Corp., who applied this methodology for oxidation of CO and H_2 [1]. Since then HTE has became *the* technology for catalyst discovery and many different reactor concepts have been developed for parallel testing of catalytic materials for a great variety of reactions [2–9]. Besides elaborated equipment, this attractive methodology also needs well-conceived theoretical reasoning. Normally, hypotheses on structure-activity/selectivity relationships are proposed to direct the catalyst design. To this end, HTE was initially combined with ex situ catalyst characterisation for obtaining knowledge about the structure of the materials. However, this approach has serious drawbacks due to the following reasons. The solids may undergo structural changes during their way from reactor to characterisation apparatus. There are differences in reaction conditions, which are caused by differences in reactor and characterisation cell design. Moreover, this classical ex situ characterisation procedure is often highly time consuming. Therefore, a new challenge in this field is to combine HTE with simultaneous catalysts characterisation under working conditions (operando approach). The term "operando" has been proposed by M.A. Bañares in August 2000 [10] as an alternative for in situ spectroscopy. The term "operando spectroscopy" describes a methodology, which combines the monitoring of the catalyst *in statu operandi* by physico-chemical techniques (evaluation of structure) and the simultaneous on-line analysis of product composition (determination of catalytic performance) in the same reactor [10–14]. The operando approach is explicitly linked to the first operando conference [15]. This research area is still under intense development and of high interest to the catalysis community [16]. The optical fibre technology in the field of heterogeneous catalysis for UV/vis spectroscopic analysis was introduced firstly by Brückner [17] and Puurunen et al. [18]. Spectral changes over the catalyst bed for the same reaction but over supported Cr catalysts are reported in [19], in which four UV/vis probes were connected to a fixed bed reactor, giving longitudinal profiles over the catalyst bed. The set-up introduced in this paper comprises a 36 channel parallel fixed bed reactor system with simultaneous UV/vis diffuse reflectance (UV/vis-DR) analysis to study changes of the catalyst structure under reaction conditions.

Against the above background, the aim of this work is to demonstrate the potential of the operando UV/vis-DR approach and its reliability for a combined HTE catalytic and spectroscopic analysis in the oxidative dehydrogenation of propane (ODP). Polycrystalline V_2O_3, VO_2, and V_2O_5 were chosen as model catalysts. As shown in a classical single channel fixed bed reactor [20], these oxides undergo reaction-induced surface and volume changes in the vanadium oxidation state during the ODP reaction

* Corresponding author. Tel.: +49 30 63924456; fax: +49 30 63924454.
E-mail address: martin.fait@catalysis.de (M.J.G. Fait).
[1] Present address: BASF Aktiengesellschaft, GCC/PP-M301 BASF SE, D-67056 Ludwigshafen, Germany.

0920-5861/$ – see front matter © 2008 Elsevier B.V. All rights reserved.
doi:10.1016/j.cattod.2008.10.023

at 500 °C. These catalyst changes can be traced by UV/vis-DR spectroscopy as shown in [20–22].

2. Experimental

2.1. Catalysts and their characterisation

VO_2 (903260, Chempur) and V_2O_5 (1.00825.0100, Merck) were commercial available, while V_2O_3 was synthesised in-house from V_2O_5 by its reduction in hydrogen according to [23]. The BET specific surface areas were determined by N_2 adsorption (77 K) using an Asap 2010 M instrument (Micromeritics). Before the BET measurements, the fresh catalysts were evacuated for 2 h at 150 °C to remove physically adsorbed water. Due to very low catalyst amounts used, the BET values of spent catalysts could not be accurately measured. XRD powder patterns were recorded on a STADI-P X-ray diffractometer (Ni-filtered Cu Kα, Stoe, Germany). The crystalline phases were identified by referring to the ICDD powder diffraction files. To calculate the vanadium oxidation state by oxygen uptake V_2O_3 and VO_2 have been oxidised to stoichiometric V_2O_5 by annealing in air at 550 °C in a crucible as described in [24].

2.2. Catalytic test conditions

The catalytic tests were performed with a $C_3H_8/O_2/N_2$ = 40/20/40 reaction feed at 500 °C and 1 bar (catalyst mass: 60 or 90 mg). Different contact times (W/F: 3–6 mg_{cat} min ml^{-1}) were achieved by varying total flow rate. After about 1 h on stream no further measurable changes in catalytic performance were observed. Then, the steady-state catalytic data were determined.

2.3. Design of the high-throughput set-up

The high-throughput set-up (Fig. 1a), whose reaction gas sampling part was originally designed and built by AMTEC (Chemnitz, Germany), operates at ambient pressure with a maximum of residence time of 8 mg_{cat} min ml^{-1} per reactor and allows fully computer controlled experiments. In the newly developed reactor module, 36 tubular reactors made of quartz are horizontally located. Three heating blocks (up to 600 °C) made of brass, each of which consists of an upper and a lower half shell, are equipped with heating cartridges.

2.4. Analytical methods for monitoring the catalytic reaction

Feed components and reaction products were analysed by an on-line micro-GC (Varian CP-2003) equipped with a suction pump and connected to the reactor system via a needle valve. With the help of a movable arm the gas samples can be taken at each individual reactor outlet. The gas chromatograph is equipped with two columns (PoraPlotQ for analysis of hydrocarbons and CO_2; Molsieve 5A for analysis of N_2, O_2, and CO) and thermal conductivity detectors. The composition of the feed gas mixture was measured in an empty reactor.

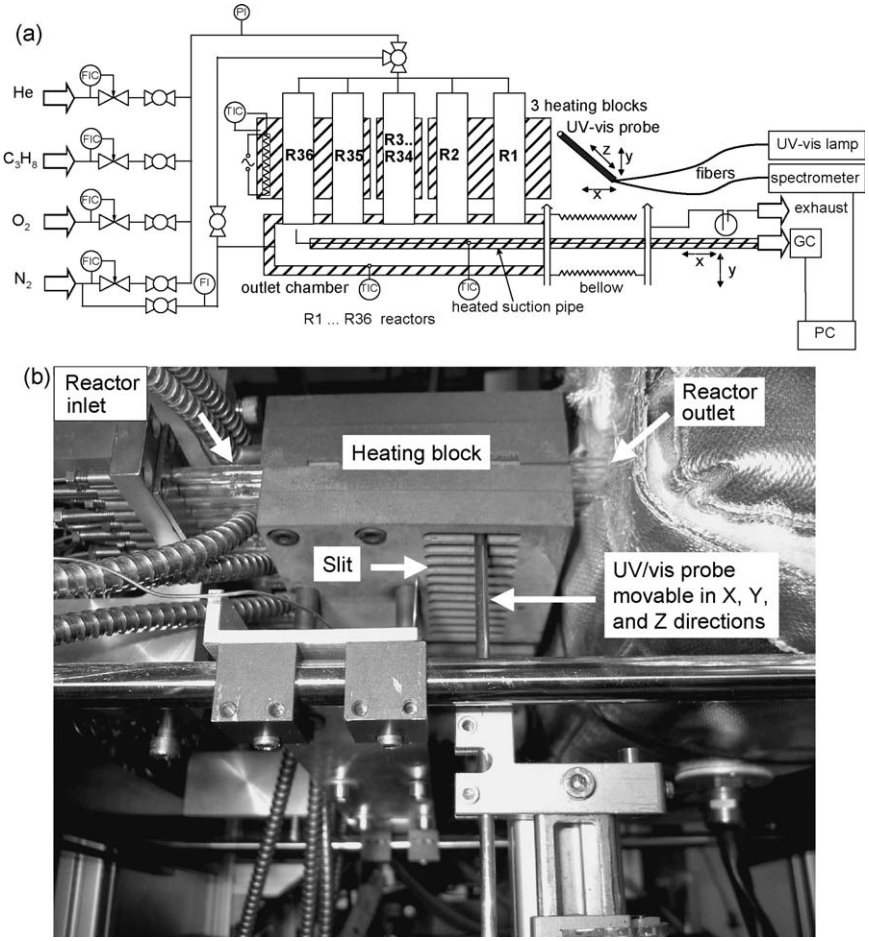

Fig. 1. Scheme (a) and picture (b) of the *operando* set-up with 36 parallel tube reactors (R1 . . . R36) for catalytic testing equipped with a gas chromatograph and an UV/vis-DR spectrometer. The picture shows the bottom side of a heating block equipped with slits, into which the movable, high temperature UV/vis probe is extending (working position).

Table 1
Reproducibility of the steady-state catalytic data of the oxidative dehydrogenation of propane ($C_3H_8/O_2/N_2$ = 40/20/40, 500 °C, W/F = 4 mg min ml^{-1}) on V_2O_5, VO_2 and V_2O_3 determined in different reactors.

	V_2O_5					VO_2					V_2O_3				
	Reactor			M^a	σ^b	Reactor			M^a	σ^b	Reactor			M^a	σ^b
	7	19	31			9	21	33			8	20	32		
$X(C_3H_8)$/%	15	16	17	16.0	1.0	4	5	5	4.7	0.7	16	16	16	16.0	0.0
$X(O_2)$/%	94	92	92	92.7	1.2	19	24	23	22.0	2.7	84	85	84	84.7	0.6
$S(C_3H_6)$/%	16	17	17	16.7	0.6	41	38	40	39.7	1.5	28	31	31	30.0	1.7
$S(CO_2)$/%	28	27	29	28.0	1.0	14	14	14	14.0	0.0	19	18	18	18.3	0.6

[a] Mean values.
[b] Standard deviations.

For operando UV/vis-DR measurements, the heating blocks are equipped with slits (5 mm width, 30 mm length) at the bottom side, in which an optical fibre probe is positioned (Fig. 1b). This probe enables to take UV/vis-DR spectra along the catalyst bed. The probe is connected via optical fibres to a UV/vis lamp and a spectrometer AvaSpec-2048 (Avantes, The Netherlands). The GC needle is movable in two dimensions (x and y direction), while the UV/vis-DR probe moves in x, y, and z direction. The three dimensions denote (i) choice of the reactor (x), (ii) movement along the catalyst bed (y), and (iii) movement of the UV/vis-DR probe near to the reactor into working position (z). The UV/vis-DR spectra were converted to the Kubelka-Munk function [25] from the reflectance R according to Eq. (1). Barium sulphate was used as a white reference material:

$$F(R) = \frac{(1-R)^2}{2R} \quad (1)$$

In order to estimate the degree of reduction of V_2O_5 under the ODP conditions, the relative Kubelka-Munk values were calculated as the ratio of the Kubelka-Munk function (R_{sample}) of the catalysts with respect to the Kubelka-Munk function of fully oxidised V_2O_5 ($R_{V_2O_5}$) according to Eq. (2) as proposed in [26]. UV/vis-DR spectra of reference V_2O_5 were recorded directly before the catalytic experiment:

$$R_{rel} = \frac{R_{sample}}{R_{V_2O_5}} \rightarrow F(R_{rel}) = \frac{(1-R_{rel})^2}{2R_{rel}} \quad (2)$$

3. Results and discussion

3.1. Characterisation of the model catalysts with respect to their initial state

The powder XRD patterns of the vanadium oxide model catalysts match excellently to PDF 71–280 (V_2O_3), PDF 43–1051 (monoclinic VO_2 stable at room temperature), and PDF 9–387 (V_2O_5) indicating that the catalysts are phase-pure. The substances are coloured: V_2O_3 is black, VO_2 is grey, while V_2O_5 is yellow-orange. The oxygen uptakes were 20.8 (theo. = 21.35) (V_2O_3) and 9.8% (9.65) (VO_2), which confirm the oxidation state of vanadium as V^{3+} (V_2O_3) and V^{4+} (VO_2), respectively. The BET specific surface areas of V_2O_3, VO_2, and V_2O_5 are relative small and amounted to 6.0, 1.7, and 7.3 $m^2\ g^{-1}$, respectively.

3.2. Temperature control of the set-up

The temperature distribution in the oven system was measured at 500 °C set point. The average temperature determined in 9 reactors at the reactor inlet was (499.3 ± 0.8) °C. Along the reactors (length: 30 mm) a temperature drop of ca. 7 K was measured resulting in an average temperature of the 9 reactors at the outlet of (493.6 ± 0.7) °C.

3.3. Reliability of the catalytic data

To demonstrate the reliability of the catalytic data three reactors were loaded with the same catalyst in each case. The steady-state performance of V_2O_5, VO_2 and V_2O_3 in the ODP reaction with W/F of 4 mg_{cat} min ml^{-1} is presented in Table 1. The low standard deviations prove the good reproducibility of the catalytic data. Therefore, the 36 channel reactor system is suitable for screening of different catalytic materials.

3.4. Reliability of the UV/vis-DR analysis

To verify the reliability of the optical unit of the 36 channel reactor system, UV/vis-DR spectra of V_2O_5 were measured in three different reactors. The spectra recorded at room temperature are presented in Fig. 2. They are characterised by two distinct absorption bands at 360 (B_{360}) and 470 nm (B_{470}), which are in line with [27–31] (the band at ca. 220 nm reported in literature could not be detected because this value is out of the range of the spectrometer). Both, bands B_{360} and B_{470} are identified as charge transfer (CT) bands [30,32–34]. d–d electron transitions can not be observed due to the electron configuration of V^{5+} ($3d^0$). Especially the energy of the band B_{470} is influenced by the number of ligands in the environment of the central ion. This band is characteristic for

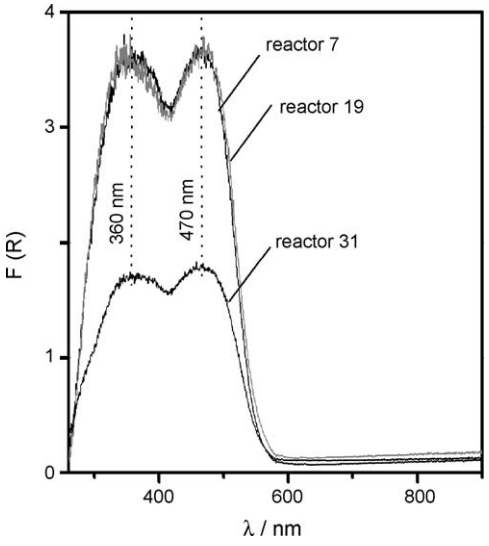

Fig. 2. UV/vis-DR spectra of V_2O_5 at room temperature in three different reactors. The absolute Kubelka-Munk values {$F(R)$} presented were calculated according to Eq. (1).

vanadium, which is coordinated octahedrally [32–34]. The band B_{360} is identified as tetrahedrally [32,33] or nearly square pyramidally coordinated V^{5+} [30]. The edge of B_{470} (turning point) at ca. 530 nm corresponds to the energy gap between the valence band of O 2*p* and the conduction band of V 3*d* [29] and causes the orange colour of V_2O_5.

The absolute positions of the B_{360} and B_{470} bands in the UV/vis-DR spectra of V_2O_5 in three different reactors match very precisely, while their intensities differ. The differences are probably due to the following experimental insufficiencies: (i) mainly mechanical adjustment of the tip of the fibre with respect to the axis of the reactor, (ii) optical irregularities of the quartz reactors, (iii) scattering phenomena at the convex reactor outer wall, and (iv) differences in reactor filling and packing density. Therefore, the absolute intensities are not comparable for the reactors among each other. However, the intensity and the band position in the UV/Vis-DR spectra are identical when the same reactor is measured repeatedly without moving the UV/vis-DR probe.

3.5. Catalytic performance of V_2O_3, VO_2 and V_2O_5

The catalytic performance of V_2O_3, VO_2 and V_2O_5 in the ODP (constant feed composition $C_3H_8/O_2/N_2 = 40/20/40$) was determined at different contact times ranging from 3 to 6 mg_{cat} min ml^{-1} (Fig. 3). Besides the main product propene the side products hydrogen, methane, ethylene and ethane as traces and carbon oxides were detected.

From Fig. 3a it could be concluded that the activity increases in the order $VO_2 < V_2O_3 \sim V_2O_5$, which corresponds with BET specific surface areas (Section 3.1). This graduation should be considered with care, because the catalysts underwent structural changes under reaction conditions (see Section 3.6), which may result in changing in specific surface areas.

Further insights into the ODP reaction over polycrystalline vanadium oxides were derived from the analysis of C_3H_6 and CO_2 selectivities at different degrees of propane conversion. The selectivity-conversion plots are shown in Fig. 3c and d. From these figures, it is obvious that there are only small differences in the selectivities between the catalysts under steady-state conditions. This conclusion agrees with previous results obtained in a classical single fixed bed reactor system [20].

3.6. Structural changes of V_2O_5 during catalytic reaction

To monitor reaction-induced changes of the V_2O_5 catalyst during the ODP reaction (constant parameters: $C_3H_8/O_2/N_2 = 40/20/40$, 500 °C, W/F = 3 mg_{cat} min ml^{-1}), operando relative UV/vis-DR spectra (not shown) were taken at the reactor inlet and outlet as a function of time on stream (ca. 13 min, time step: 10 s). The relative UV/vis-DR spectra under the reaction conditions were related to that of fully oxidised V_2O_5 according to Eq. (2). In order to avoid any misunderstanding in the terminology of UV/vis-DR analysis, the spectra calculated from Eq. (2) are called as relative UV/vis-DR spectra. These relative spectra are characterised by a pre-edge UV and post-edge visible region, which are separated at the wavelength of ca. 550 nm (the absorption edge of V_2O_5, which corresponds to the energy gap between valence and conduction bands). The relative UV/vis-DR spectra of V_2O_5 at the reactor outlet are characterised by a band at 700 nm. Its intensity increases with time on stream. The relative UV/vis-DR spectra of V_2O_5 at the reactor inlet show bands at ca. 520 and ca. 740 nm. The time resolved band intensities for the inlet and outlet spectra at 520 and 700/740 nm over a period of ca. 13 min are exemplified in Figs. 4a

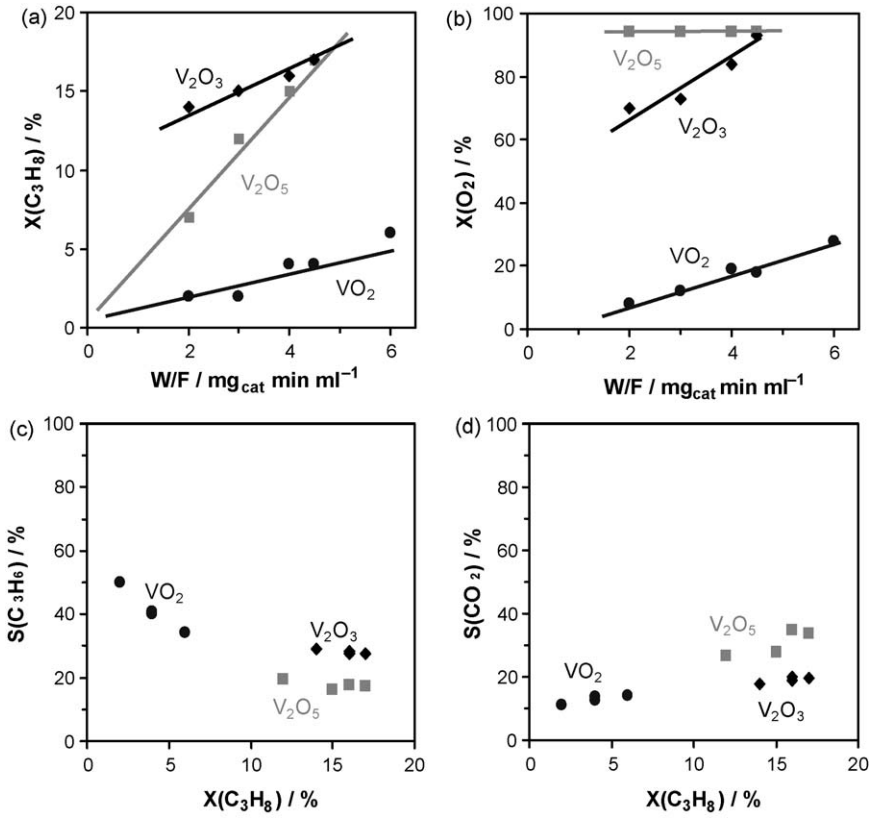

Fig. 3. Steady-state catalytic performance of V_2O_5, VO_2 and V_2O_3 in the oxidative dehydrogenation of propane (500 °C, $C_3H_8/O_2/N_2 = 40/20/40$), propane (a) and oxygen conversions (b) at different contact times (W/F), selectivities to C_3H_6 (c) and CO_2 (d) determined at different degrees of propane conversion.

and b. For their interpretation, the relative spectra of VO_2 and V_2O_3 at 500 °C in N_2 are given in Fig. 4c, which are very similar to each other and are dominated by a distinct signal in the visible region (d–d transitions). As expected no band is observable in the UV region. By means of the UV/vis-DR spectra it is not possible to distinguish between V^{3+} and V^{4+}.

The time-on-stream changes in the relative UV/vis-DR spectra (Fig. 4a and b) differ with respect to their point of registration along the catalyst bed. Whereas these spectra at the reactor outlet (Fig. 4b) are characterised by a temporal increase in intensity in the post-edge region (band at 700 nm), the relative spectra taken at the reactor inlet (Fig. 4a) show changes in intensity in the visible (band at 740 nm) as well as in the post-edge region (band at 520 nm). The intensity in the region around 740 nm increases in the first minute and than drops again to reach a constant value after about 2 min. At the point of maximum intensity at 1 min a band at 520 nm appears, whose intensity remains nearly constant after 2.5 min TOS. It should be stressed that the time-on-stream changes observed under the ODP conditions should be interpreted qualitatively only. Therefore, no quantitative conclusions can be drawn from the below discussion.

This change of intensity with time-on-stream can be interpreted as follows. The spectra recorded at the outlet are very similar to pure VO_2 and V_2O_3 and so it is to conclude that either VO_2 or V_2O_3 or both phases are formed. The ex situ XRD pattern (not shown) of this sample matches excellently to V_2O_3 (PDF 84–316). Hence, the increase of the band intensity at 700 nm with TOS indicates in combination with the XRD phase analysis the complete reduction of the initial V_2O_5 to V_2O_3 at the reactor outlet. This is plausible, because oxygen is completely consumed (Fig. 3b), while the degree of propane conversion is below 20%. Therefore, the catalyst is exposed to a strongly reducing atmosphere favouring reduction of V_2O_5 to V_2O_3. The increase in signal intensity at 740 nm is due to the reduction of the initial V^{5+} ions to V^{4+} or V^{3+}. Keeping in mind that the feed contains 20% oxygen at the reactor inlet we have a more oxidative atmosphere as compared to the reactor outlet where the oxygen is completely consumed (Fig. 3b). So, it is likely that firstly V^{4+} is formed. The evolution of the band at 520 nm caused by CT transitions and characteristic for octahedral V^{5+} (cf. Section 3.4) indicates the formation of oxidised species. This hypothesis is confirmed by two observations: (i) the XRD crystalline phase analysis reveals besides V_2O_3 mainly VO_2 (PDF 73–2362) and small amounts of $V_{12}O_{26}$ (PDF 72–1278) with an average vanadium oxidation state of $V^{4.3+}$ and (ii) a catalyst zone at the reactor inlet is coloured like pure VO_2 (grey-black) as compared to the rest of the catalyst bed, which is black (like pure V_2O_3).

This result implies that an equilibrium state with respect to the vanadium oxidation state is achieved during approx. 8 min TOS. This agrees roughly with data published in [26], where during the first 6 min after starting the ODP reaction on a 10 wt% V_2O_5/Al_2O_3 catalyst (but note that the reaction conditions applied differ from ours: $C_3H_8/O_2/Ar$ = 13.8/1.7/84.5, 330 °C) the intensity of the absorbance in the post-edge region increased markedly, whereas the absorption in the pre-edge region decreased. Then, both spectrum features stay nearly unchanged over ca. 2 h on stream. From these findings, it is to conclude that catalyst zones with different composition exist, at least at the inlet and outlet. The formation of such zones differentiated by their colour and, therefore, by their vanadium oxidation states was reported for the ODP reaction over a V_2O_5 bulk catalyst [35] at reaction conditions, which, however, are not comparable to the ones applied here.

It is well accepted, that propane and oxygen react in the ODP reaction with vanadium ions from the catalyst according to the Mars–van Krevelen mechanism. From our findings concerning the

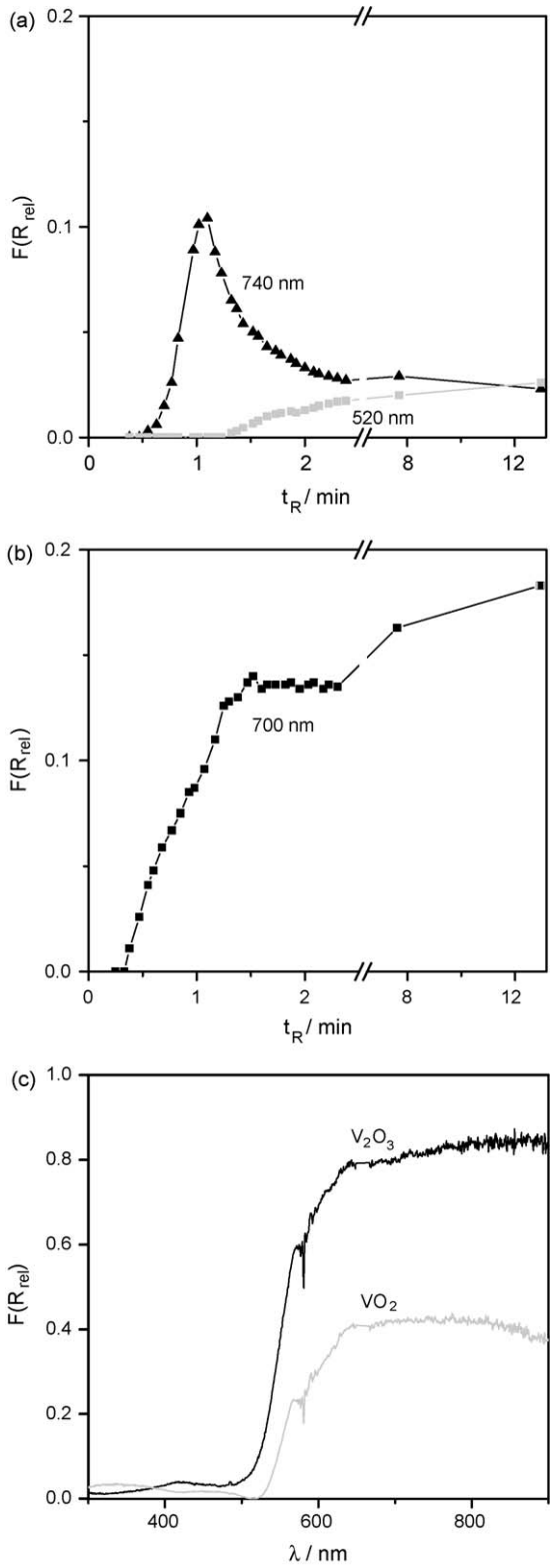

Fig. 4. Changes of the band intensities deduced from the relative UV/vis-DR spectra {given as $F(R_{rel})$ and calculated according to Eq. (2)} of V_2O_5 at 500 °C at the respective wavelengths (540, 700, and 740 nm) in dependence of time on stream of oxidative dehydrogenation of propane ($C_3H_8/O_2/N_2$ = 40/20/40, W/F = 3 mg_{cat} min ml^{-1}) for the reactor inlet (a) and the outlet (b). As reference the relative UV/vis-DR spectra at 500 °C of V_2O_3 and VO_2 in N_2 relative to V_2O_5 (Eq. (2)) are depicted in (c).

reduction of the V^{5+} ions it follows that the composition of the reaction feed varies along the catalyst bed, and oxygen and propane are consumed in different extent. Thus, the catalyst works at different conditions. Whereas the reaction feed with a stoichiometric ratio of propane to oxygen (C_3H_8:O_2 = 2:1) is depleted in both reactants in minor extent at the inlet, in the mid and outlet oxygen and propane consumption is higher probably according to their steady-state conditions (X(O_2): > 90%, X(C_3H_8): ca. 12%). Moreover, propene is enriched along the catalyst bed. That has the consequence that at the mid the reaction feed is more reducing in contrast to the inlet, where its reducing power is moderated because here propane and oxygen coexist. These differences in reducing power of reaction feed in dependence of axial position of the catalyst bed explains why vanadium is stronger reduced at the outlet of the catalyst bed than at the inlet at least at the reaction conditions chosen.

4. Conclusions

A novel 36 channel high-throughput catalytic testing device combined with operando UV/vis diffuse reflectance spectroscopy was developed. This reactor system enables to determine simultaneously the catalytic performance and to monitor the changes of the catalyst under real reaction conditions (e.g. temperature, partial pressures and catalyst particles). Its potential and reliability were successfully demonstrated for the ODP over polycrystalline vanadium oxide catalysts (V_2O_3, VO_2 and V_2O_5). The catalytic data are comparable with those previously determined in a classical single fixed bed reactor system [20].

The coupling of catalytic measurements and UV/vis-DR spectroscopy presented in this work demonstrates impressively the capabilities of the operando methodology. The advantage of the UV/vis-DR spectroscopy is its speed to trace catalyst restructuring during catalytic reaction. So, the catalyst working behaviour under reaction conditions could be studied and vanadium species in different oxidation states along the catalyst bed could be identified. In that way deeper insights into the vanadia catalysed ODP reaction could be quickly revealed. In general this reactor system can be applied for different gas-phase solid reactions, where catalytic materials undergo redox changes under reaction conditions. Moreover, it can be also used for monitoring of coke formation as well as to trace certain calcination or reduction procedures.

Acknowledgements

The authors thank P. Max for technical assistance and improving the control hardware and software, R. Eckelt for preparation of V_2O_3 samples as well as for technical assistance and the Federal Ministry of Education and Research, Germany, the State of Berlin, and the EU (European Fund for Regional Developement, project EFRD 2000 2005 1/0) for financial support. EVK would like to thank the Deutsche Forschungsgemeinschaft (DFG) within the frame of the competence network (Sonderforschungsbereich 546) "Structure, dynamics and reactivity of transition metal oxide aggregates".

References

[1] W.H. Weinberg, B. Jandeleit, K. Self, H. Turner, Curr. Opin. Solid State Mater. Sci. 3 (1998) 104.
[2] P. Cong, R. Doolen, Q. Fan, D. Giaquinta, S. Guan, E. McFarland, D.M. Poojary, K. Self, H.W. Turner, W.H. Weinberg, Angew. Chem. 111 (1999) 507.
[3] Patent WO0019990641 60A1 (1999) to Symyx Technologies.
[4] U. Rodemerck, P. Ignaszewski, M. Lukas, P. Claus, Chem. Eng. Technol. 23 (2000) 413.
[5] S. Geisler, I. Vauthey, D. Farusseng, H. Zanthoff, M. Muhler, Catal. Today 81 (2003) 413.
[6] R.J. Hendershot, S.S. Lasko, M.F. Fellmann, G. Oskarsdottir, W.N. Delgass, C.M. Snively, J. Lauterbach, Appl. Catal. A: Gen. 254 (2003) 107.
[7] F. Schüth, L. Baumes, F. Clerc, D. Demuth, D. Farrusseng, J. Llamas-Galilea, C. Klanner, J. Klein, A. Martinez-Joaristi, J. Procelewska, Catal. Today 117 (2006) 284.
[8] F. Schüth, D. Demuth, Chem. Eng. Technol. Ing. Tech. 78 (2006) 851.
[9] Y. Yamada, T. Kobayashi, J. Jpn. Petrol. Inst. 49 (2006) 157.
[10] B.M. Weckhuysen, Chem. Commun. (2002) 97.
[11] M.A. Bañares, M.O. Guerrero-Perez, J.L.G. Fierro, G.G. Cortez, J. Mater. Chem. 12 (2002) 3337.
[12] M.A. Bañares, Catal. Today 100 (2005) 71.
[13] A. Brückner, E. Kondratenko, Catal. Today 113 (2006) 16.
[14] M.A. Bañares, I.E. Wachs, J. Raman Spectrosc. 33 (2002) 359.
[15] B.M. Weckhuysen, Phys. Chem. Chem. Phys. 5 (2003) 4351.
[16] Catal. Today 126 (2007), Special issue containing contributions of the 2nd International Congress on Operando Spectroscopy, Toledo, Spain (April 23–27, 2006), http://www.aca-berlin.de/operando.
[17] A. Brückner, Chem. Commun. (2001) 2122.
[18] R.L. Puurunen, B.G. Beheydt, B.M. Weckhuysen, J. Catal. 204 (2001) 253.
[19] T.A. Nijhuis, S.J. Tinnemans, T. Visser, B.M. Weckhuysen, Chem. Eng. Sci. 59 (2004) 5487.
[20] E.V. Kondratenko, O. Ovsitser, J. Radnik, M. Schneider, R. Kraehnert, U. Dingerdissen, Appl. Catal. A: Gen. 319 (2007) 98.
[21] L. Burcham, G. Deo, X. Gao, I. Wachs, Top. Catal. 11–12 (2000) 85.
[22] X. Gao, J.M. Jehng, I.E. Wachs, J. Catal. 209 (2002) 43.
[23] G. Brauer, Handbuch der Präparativen Anorganischen Chemie, Ferdinand Enke Verl, Stuttgart, 1962.
[24] O. Grossmann, H. Oppermann, W. Reichelt, Z. Chem. 16 (1976) 289.
[25] G. Kortüm, Reflexionsspektroskopie, Springer, Berlin, Heidelberg, New York, 1969
[26] M.D. Argyle, K. Chen, C. Resini, C. Krebs, A.T. Bell, E. Iglesia, J. Phys. Chem. B 108 (2004) 2345.
[27] F. Vratny, F. Micale, Trans. Faraday Soc. 59 (1963) 2739.
[28] H. Praliaud, M.-V. Methieu, J. Chim. Phys. 73 (1976) 509.
[29] T. Tanaka, Y. Nishimura, S.I. Kawasaki, M. Ooe, T. Funabiki, S. Yoshida, J. Catal. 118 (1989) 327.
[30] G. Centi, S. Perathoner, F. Trifiro, A. Aboukais, C.F. Aissi, M. Guelton, J. Phys. Chem. 96 (1992) 2617.
[31] X.T. Gao, I.E. Wachs, J. Phys. Chem. B 104 (2000) 1261.
[32] W. Hanke, R. Bienert, H.-G. Jerschkewitz, Z. Anorg. Allg. Chem. 414 (1975) 109.
[33] G. Lischke, W. Hanke, H.-G. Jerschkewitz, G. Ohlmann, J. Catal. 91 (1985) 54.
[34] M. Schraml-Marth, A. Wokaun, M. Pohl, H.-L. Krauss, J. Chem. Soc., Faraday Trans. 87 (1991) 2635.
[35] B.P. Barbero, L.E. Cadus, L. Hilaire, Appl. Catal. A: Gen. 246 (2003) 237.